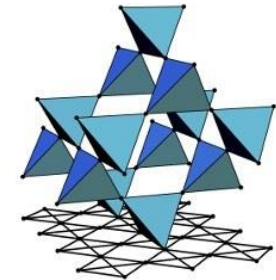




TECHNISCHE
UNIVERSITÄT
DRESDEN

DRESDEN
concept



SFB 1143

Tensor network representations of parton wave functions

Hong-Hao Tu

In collaboration with Ying-Hai Wu (HUST, China)
Lei Wang (IOP, China)

Y.-H. Wu, L. Wang & HHT, arXiv:1910.11011

Entanglement in Strongly Correlated Systems
Benaque, February 21st, 2020

Background

- Parton wave functions have been extensively used as variational ansatz in strongly correlated systems (e.g. high- T_c , quantum Hall, spin liquids).

Example: fermionic/bosonic representation for spin-1/2

$$\vec{S}_j = \frac{1}{2} \sum_{\alpha\beta=\uparrow,\downarrow} c_{j\alpha}^\dagger \vec{\sigma}_{\alpha\beta} c_{j\beta}$$

constraint: $\sum_{\alpha=\uparrow,\downarrow} c_{j\alpha}^\dagger c_{j\alpha} = 1$

$$|\psi\rangle = P_G \prod_{|\mathbf{k}| < k_F} \prod_{\alpha=\uparrow,\downarrow} c_{\mathbf{k}\alpha}^\dagger |0\rangle$$

$$|\psi\rangle = P_G \exp \left[\sum_{j < l} g_{jl} (c_{j\uparrow}^\dagger c_{l\downarrow}^\dagger - c_{j\downarrow}^\dagger c_{l\uparrow}^\dagger) \right] |0\rangle$$

P_G : Gutzwiller projector (imposing the local constraint)

Background

- General construction: fermionic/bosonic Gaussian states subject to local projections
- Parton wave functions are determinant/Pfaffian/permanent wave functions (numerical technique: Variational Monte Carlo).

- Advantage:**
- Physically motivated (with very few parameters)
 - (Possible) connection to low-energy effective theory
- Drawback:**
- Computationally expensive (sometimes impossible, e.g. most bosonic RVB states => permanent)
 - Characterization tools rare (e.g. entanglement spectrum/entropy not available)

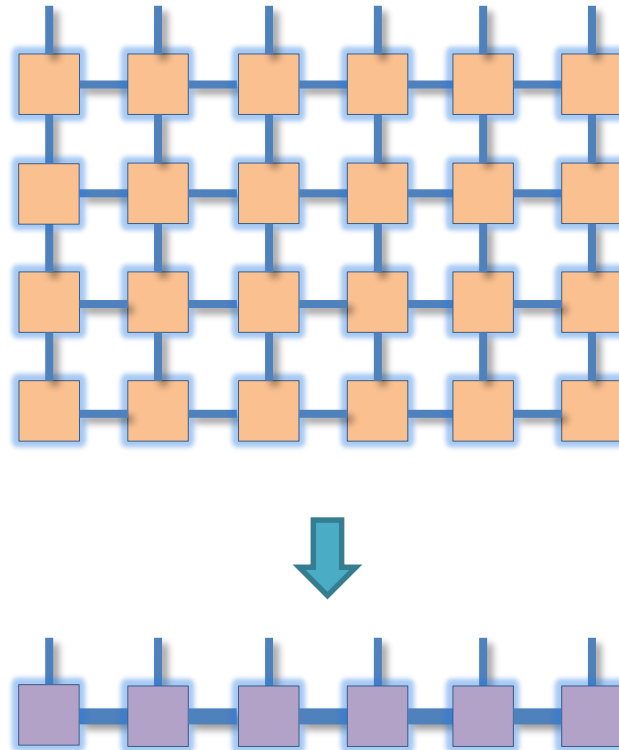
Representing parton wave functions as tensor networks

This talk:

- Derive exact tensor network representations
- Compress tensor networks into Matrix Product States

Motivation:

- Computations and characterizations become easy/possible
- Good ansatz for initializing DMRG



Gutzwiller projected Fermi sea

Example:

$$|\psi\rangle = P_G \prod_{m=1}^N d_m^\dagger |0\rangle$$

Occupied single-particle orbitals:

$$d_m^\dagger = \sum_{j=1}^N \sum_{\alpha=\uparrow,\downarrow} A_{m,j\alpha} c_{j\alpha}^\dagger = \sum_{l=1}^{2N} A_{ml} c_l^\dagger$$

$\xrightarrow{\hspace{1cm}}$
 $l = (j, \alpha)$

$l = 1$ $l = 2$ \dots



$j = 1, \alpha = \uparrow$ $j = 1, \alpha = \downarrow$ \dots

Single-particle orbital as Matrix Product Operator

$$\begin{aligned} d_m^\dagger &= \sum_{l=1}^{2N} A_{ml} c_l^\dagger \\ &= (0 \quad 1) \begin{pmatrix} 1 & 0 \\ A_{m1} c_1^\dagger & 1 \end{pmatrix} \begin{pmatrix} 1 & 0 \\ A_{m2} c_2^\dagger & 1 \end{pmatrix} \cdots \begin{pmatrix} 1 & 0 \\ A_{m,2N} c_{2N}^\dagger & 1 \end{pmatrix} \begin{pmatrix} 1 \\ 0 \end{pmatrix} \end{aligned}$$

Single-particle orbital as Matrix Product Operator

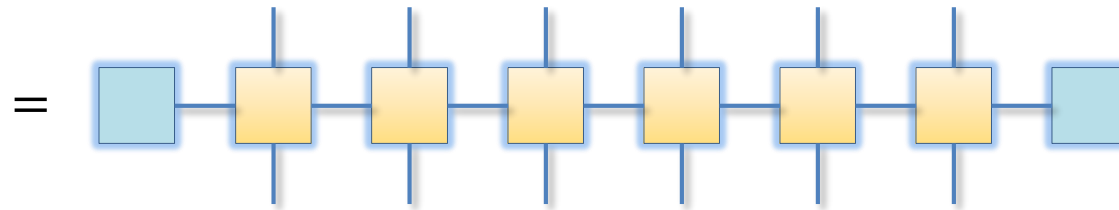
$$\begin{aligned} d_m^\dagger &= \sum_{l=1}^{2N} A_{ml} c_l^\dagger \\ &= (0 \quad 1) \begin{pmatrix} 1 & 0 \\ A_{m1} c_1^\dagger & 1 \end{pmatrix} \begin{pmatrix} 1 & 0 \\ A_{m2} c_2^\dagger & 1 \end{pmatrix} \cdots \begin{pmatrix} 1 & 0 \\ A_{m,2N} c_{2N}^\dagger & 1 \end{pmatrix} \begin{pmatrix} 1 \\ 0 \end{pmatrix} \\ &= (0 \quad 1) \begin{pmatrix} 1 & 0 \\ A_{m1} \sigma_1^+ & \sigma_1^z \end{pmatrix} \begin{pmatrix} 1 & 0 \\ A_{m2} \sigma_2^+ & \sigma_2^z \end{pmatrix} \cdots \begin{pmatrix} 1 & 0 \\ A_{m,2N} \sigma_{2N}^+ & \sigma_{2N}^z \end{pmatrix} \begin{pmatrix} 1 \\ 0 \end{pmatrix} \end{aligned}$$

Jordan-Wigner mapping: $c_l^\dagger = \sigma_1^z \cdots \sigma_{l-1}^z \sigma_l^+$

Single-particle orbital as Matrix Product Operator

$$d_m^\dagger = \sum_{l=1}^{2N} A_{ml} c_l^\dagger$$

$$= (0 \quad 1) \begin{pmatrix} 1 & 0 \\ A_{m1}\sigma_1^+ & \sigma_1^z \end{pmatrix} \begin{pmatrix} 1 & 0 \\ A_{m2}\sigma_2^+ & \sigma_2^z \end{pmatrix} \cdots \begin{pmatrix} 1 & 0 \\ A_{m,2N}\sigma_{2N}^+ & \sigma_{2N}^z \end{pmatrix} \begin{pmatrix} 1 \\ 0 \end{pmatrix}$$



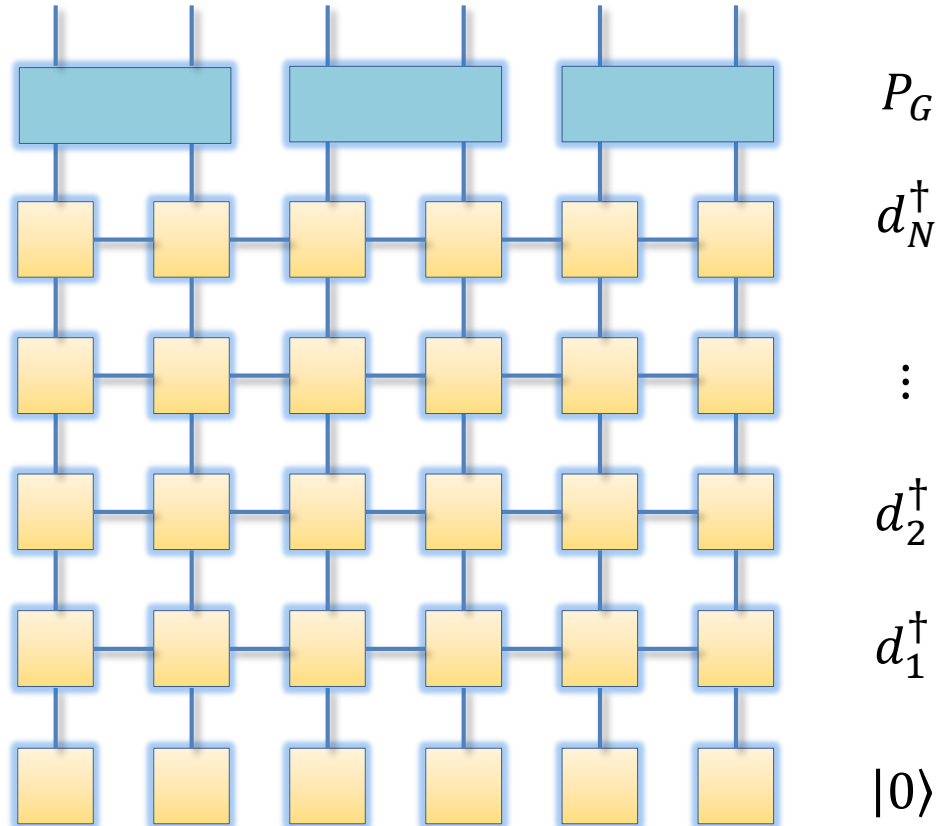
$$\begin{array}{ccccc} 1 & \square & 1 & = & 1 \\ & | & & & | \\ & \square & & & \square \\ & | & & & | \\ 2 & \square & 2 & = & \sigma^z \\ & | & & & | \\ & \square & & & \square \\ & | & & & | \\ 2 & \square & 1 & = & A_{ml}\sigma^+ \\ & | & & & | \end{array}$$

Tensor network representation of Fermi sea

$$\prod_{m=1}^N d_m^\dagger |0\rangle = \begin{array}{c} \text{Diagram of a 2D tensor network: } \\ \text{A grid of } N \times N \text{ yellow squares (tensors) connected by blue lines (edges).} \\ \text{The network is fully connected horizontally and vertically.} \\ \text{Vertical edges connect the bottom row to the top row.} \\ \text{The rightmost column of tensors is labeled: } \\ d_N^\dagger & \vdots & d_2^\dagger & d_1^\dagger & |0\rangle \end{array}$$

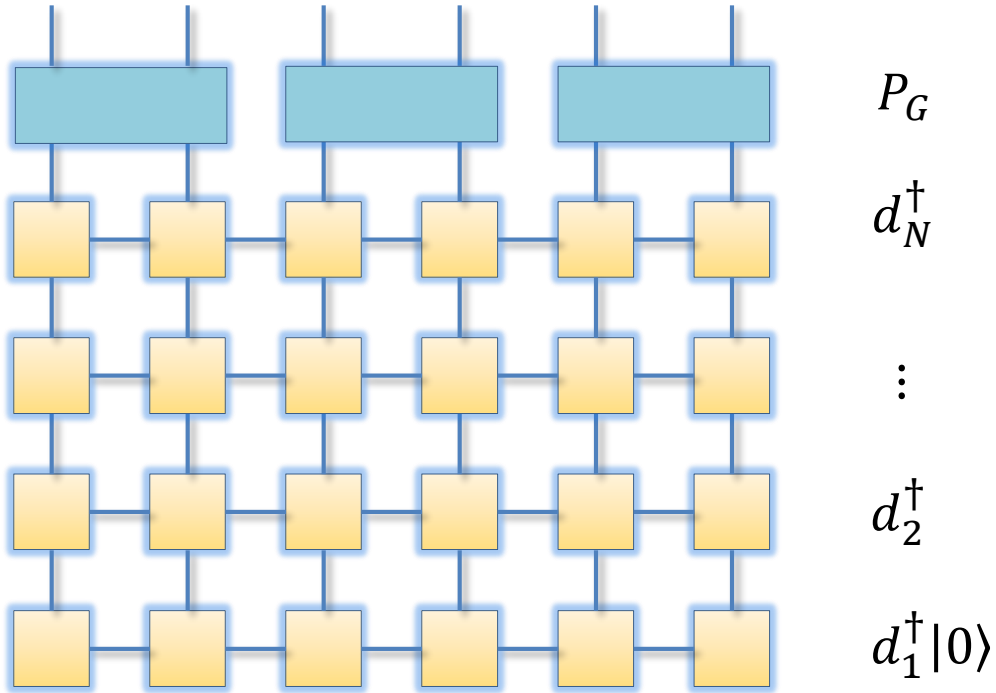
Tensor network representation of projected Fermi sea

$$P_G \prod_{m=1}^N d_m^\dagger |0\rangle =$$



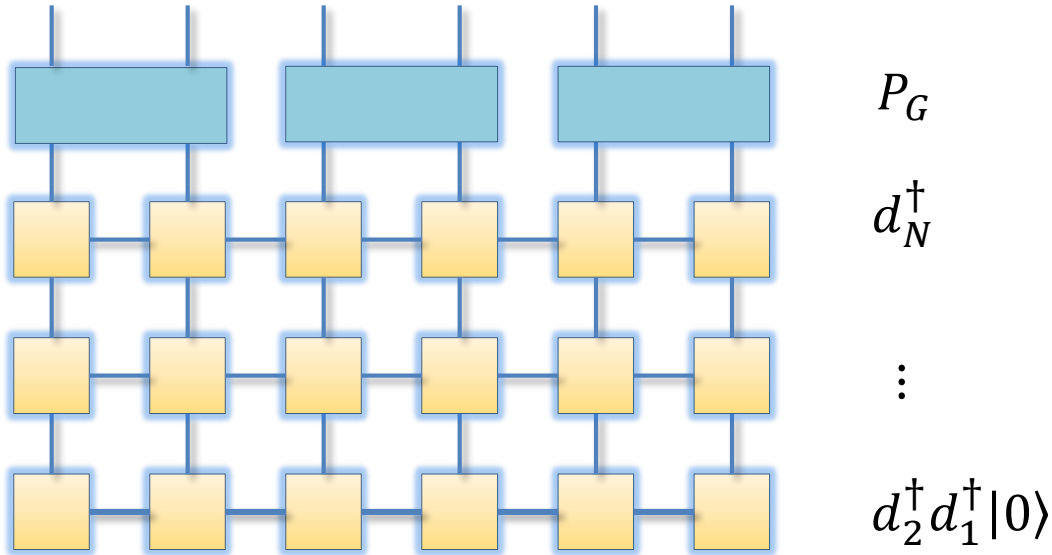
Compressing MPO-MPS tensor network into MPS

$$P_G \prod_{m=1}^N d_m^\dagger |0\rangle =$$



Compressing MPO-MPS tensor network into MPS

$$P_G \prod_{m=1}^N d_m^\dagger |0\rangle =$$



Compressing MPO-MPS tensor network into MPS

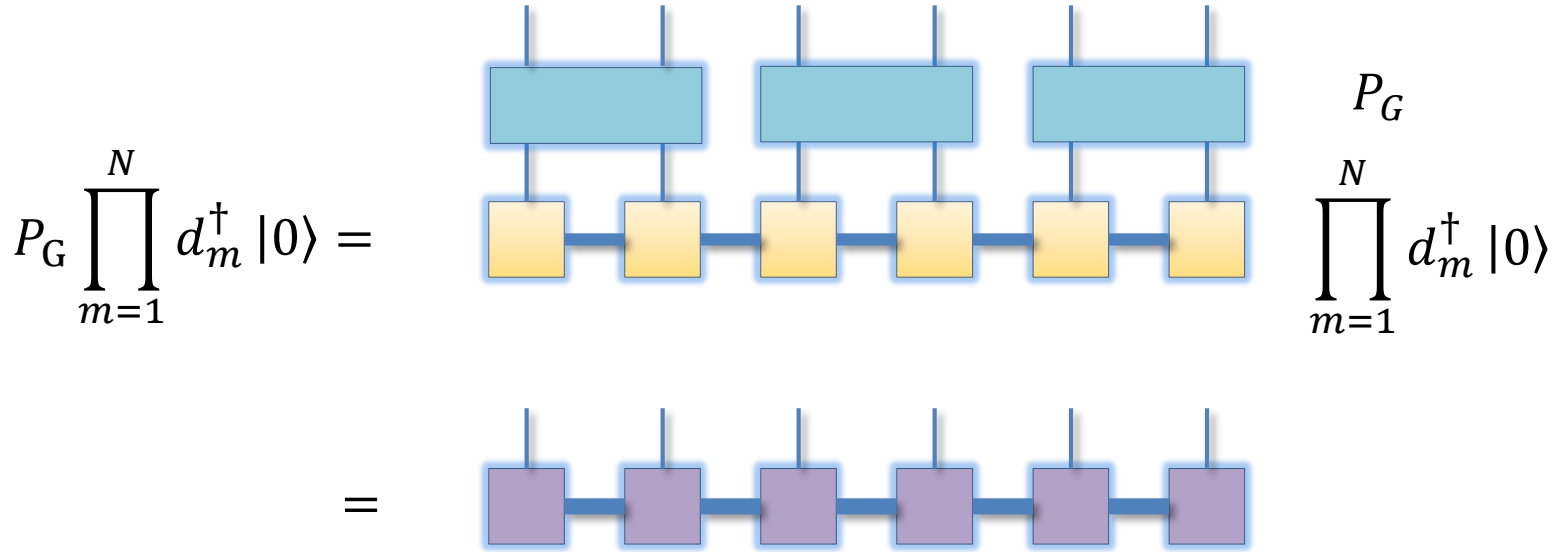
$$P_G \prod_{m=1}^N d_m^\dagger |0\rangle = \begin{array}{c} \text{Diagram of a 3-layer MPS tensor network:} \\ \text{Top layer (blue boxes)} \\ \text{Middle layer (yellow boxes)} \\ \text{Bottom layer (yellow boxes)} \\ \text{Horizontal connections between adjacent sites in the middle and bottom layers} \\ \text{Vertical connections from top to middle, middle to bottom, and bottom to output} \end{array} P_G \dots d_3^\dagger d_2^\dagger d_1^\dagger |0\rangle$$

Compressing MPO-MPS tensor network into MPS

$$P_G \prod_{m=1}^N d_m^\dagger |0\rangle = \text{Diagram} = P_G \prod_{m=1}^N d_m^\dagger |0\rangle$$

The diagram illustrates the compression of an MPO-MPS tensor network into an MPS. It consists of three horizontal layers of tensors. The top layer contains three light blue rectangular blocks, each with two vertical blue lines extending upwards from its top edge. The middle layer contains three light yellow rectangular blocks, each with two vertical blue lines extending downwards from its bottom edge. The bottom layer contains a single horizontal blue line connecting the three yellow blocks. This structure represents the compressed MPS form of the original MPO-MPS network.

Compressing MPO-MPS tensor network into MPS



- Truncation needed in intermediate steps



High fidelity compression requires low-entanglement
“intermediate” states!

Maximally localized Wannier orbitals

$$\prod_{m=1}^N d_m^\dagger |0\rangle = \prod_{r=1}^N f_r^\dagger |0\rangle$$

Wannier orbitals $f_r^\dagger = \sum_{m=1}^N B_{rm} d_m^\dagger = \sum_{l=1}^{2N} (BA)_{rl} c_l^\dagger$

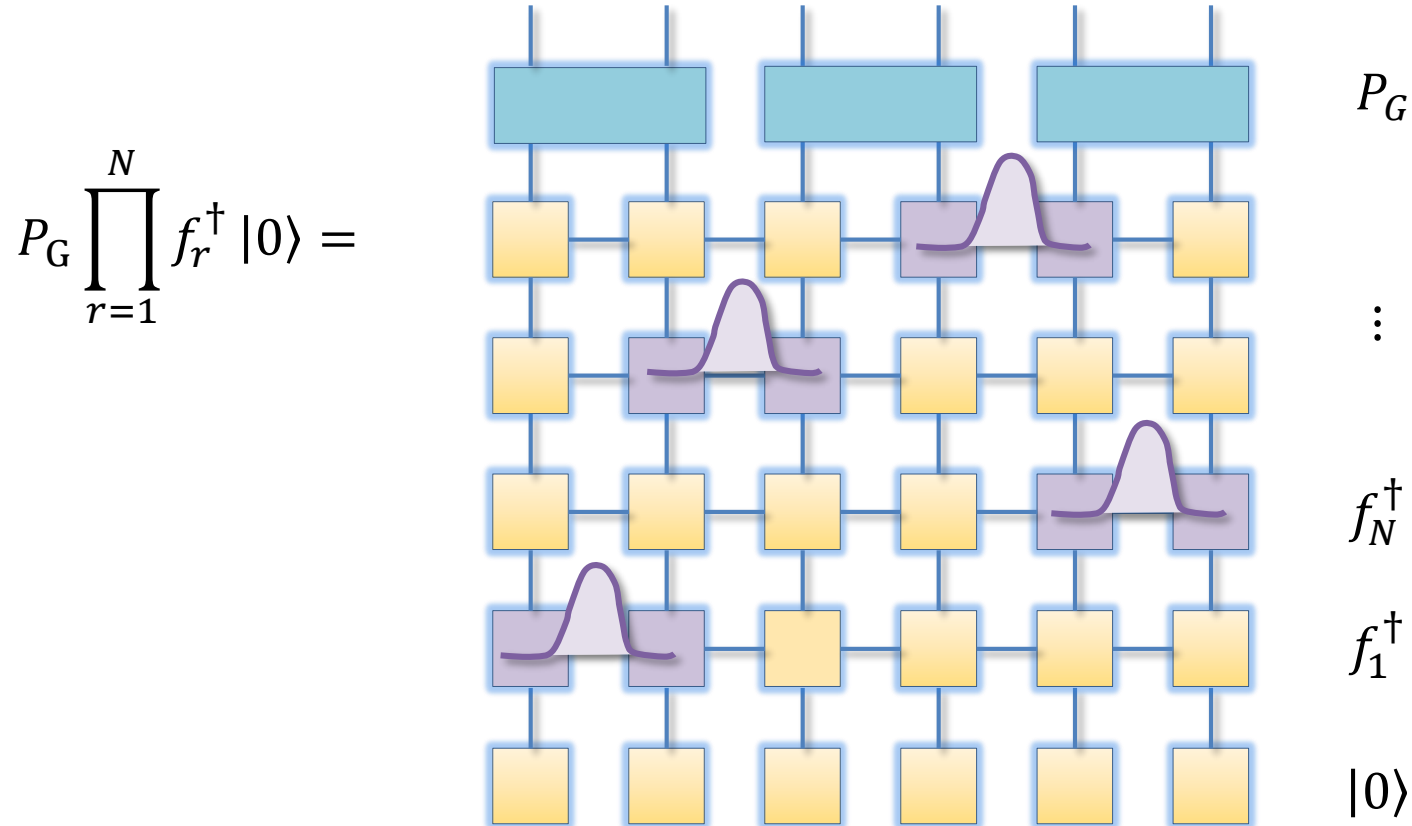
- Determination of maximally localized Wannier orbitals:

Position operator: $X = \sum_{l=1}^{2N} l c_l^\dagger c_l$

Diagonalization of the “projected”
position operator (within the subspace
of occupied single-particle states) $\rightarrow f_r^\dagger$

$$X_{mn} = \langle 0 | d_m X d_n^\dagger | 0 \rangle$$

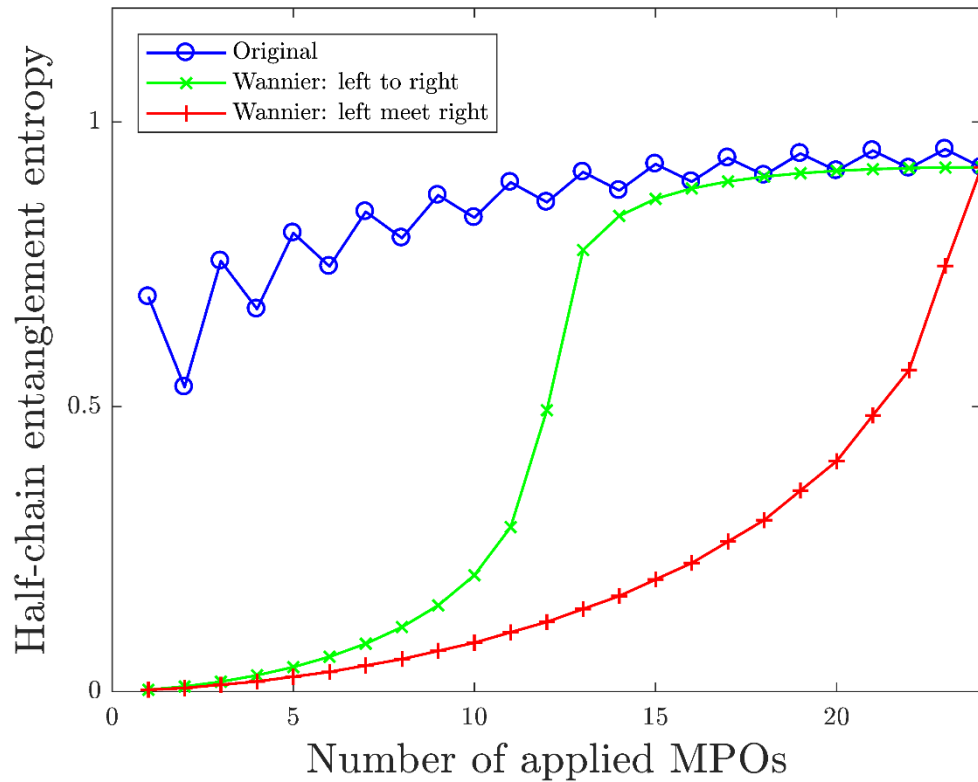
Compression with Wannier orbitals: left-meet-right



- Accelerated MPO-MPS evolution and substantially suppressed truncation errors (due to **gradually** built-up entanglement)!

Example: 1D half-filled Fermi sea with OBC

$$d_m^\dagger = \sqrt{\frac{2}{N+1}} \sum_{j=1}^N \sin\left(\frac{\pi m j}{N+1}\right) c_j^\dagger \quad 1 \leq m \leq N/2$$



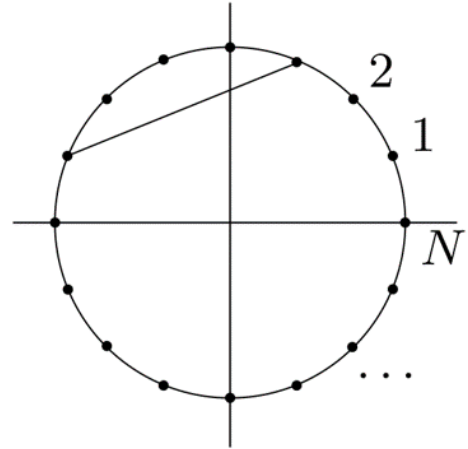
Benchmark: 1D Haldane-Shastry model

$$|\psi\rangle = P_G \prod_{|k|<\pi/2} \prod_{\alpha=\uparrow,\downarrow} c_{k\alpha}^\dagger |0\rangle$$

- Ground state of the Haldane-Shastry model

$$H_{\text{HS}} = \sum_{i < j} \frac{\vec{S}_i \cdot \vec{S}_j}{\left(\frac{N}{\pi}\right)^2 \sin^2 \frac{\pi}{N} (i - j)}$$

with energy $E_{\text{GS}} = -\frac{\pi^2}{24} \left(N + \frac{5}{N}\right)$



F.D.M. Haldane, PRL (1988);
B.S. Shastry, PRL (1988).

- Benchmark: $N = 100$, $E_{\text{GS}} = -41.1439133\dots$

MPS: $D = 1000$, $E = -41.1435412\dots$

$D = 3000$, $E = -41.1439061\dots$

$D = 5000$, $E = -41.1439125\dots$

$\rightarrow \left| \frac{E - E_{\text{GS}}}{E_{\text{GS}}} \right| \sim 10^{-7}$

Benchmark: 2D Laughlin chiral spin liquid

- Parton “mean-field” Hamiltonian:

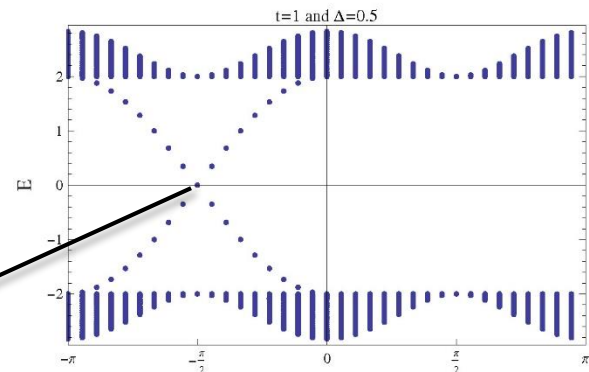
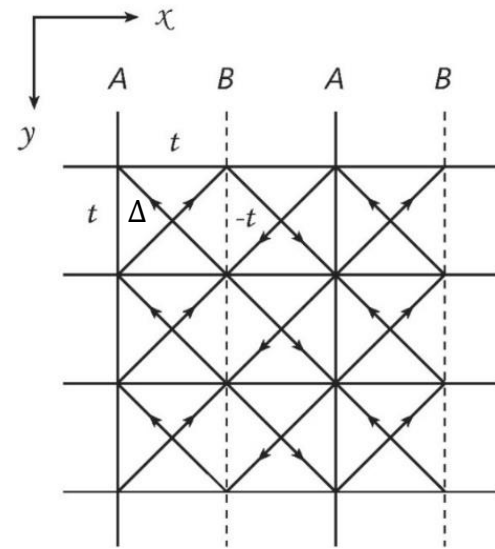
$$H_{\text{MF}} = \sum_{\langle ij \rangle, \alpha} t_{ij} c_{i\alpha}^\dagger c_{j\alpha} + \sum_{\langle\langle ij \rangle\rangle, \alpha} \Delta_{ij} c_{i\alpha}^\dagger c_{j\alpha}$$

- Parton wave functions of **two** topological sectors (**identity & semion**) on a **cylinder**:

$$|\psi_I\rangle = P_G \gamma_{L\uparrow}^\dagger \gamma_{L\downarrow}^\dagger |\text{FS}\rangle$$

$$|\psi_s\rangle = P_G \gamma_{L\uparrow}^\dagger \gamma_{R\downarrow}^\dagger |\text{FS}\rangle$$

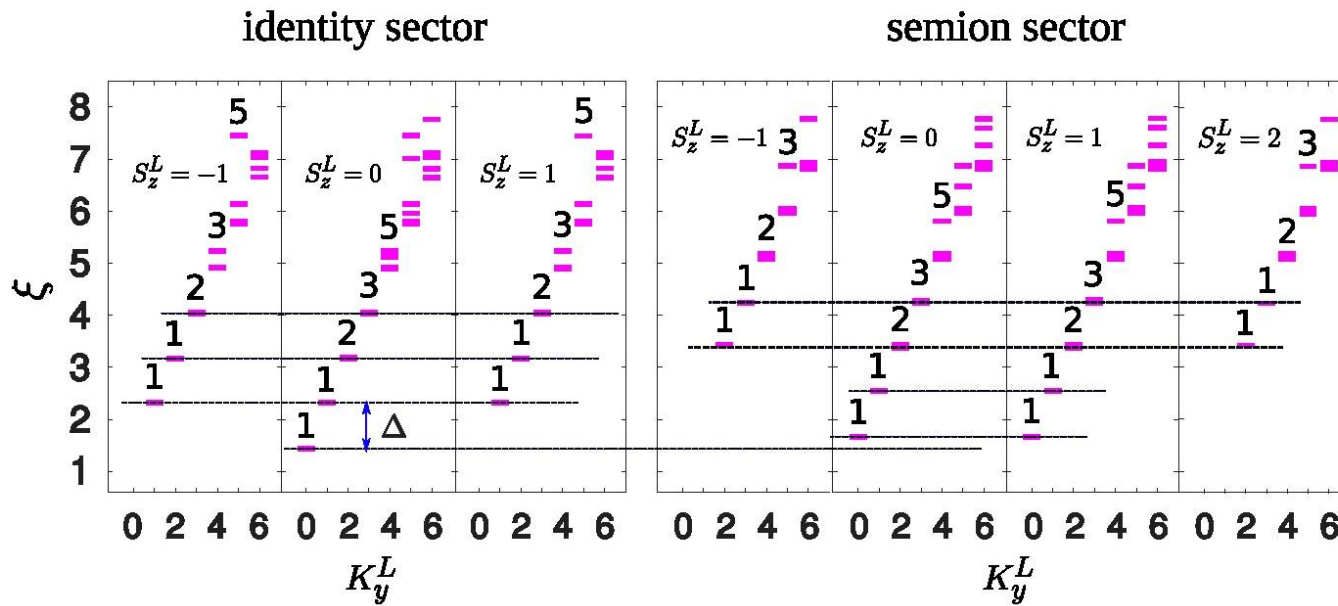
$\gamma_{L\alpha}^\dagger$ and $\gamma_{R\alpha}^\dagger$



Benchmark: 2D Laughlin chiral spin liquid

Benchmark: $N_x = 16, N_y = 10$

MPS: $D = 9000$



- Entanglement spectrum agrees with the $SU(2)_1$ CFT
- Topological spin of semion: $h_s \approx 0.2617$ (expected: $h_s = 1/4$)

Summary and outlook

- We have obtained exact tensor network representations of parton wave functions.
- For the projected Fermi sea, maximally localized Wannier orbitals allow a high-fidelity compression into MPS.
(See H.-K. Jin, HHT & Y. Zhou, arXiv:2001.04611 for projected BCS states)
- Outlook: Projected bosonic paired states (bosonic RVB), continuum limit, excitations...

Summary and outlook

- We have obtained exact tensor network representations of parton wave functions.
- For the projected Fermi sea, maximally localized Wannier orbitals allow a high-fidelity compression into MPS.
(See H.-K. Jin, HHT & Y. Zhou, arXiv:2001.04611 for projected BCS states)
- Outlook: Projected bosonic paired states (bosonic RVB), continuum limit, excitations...

Thank you for your attention!